Direct evidence of the impact of aqueous self-assembly on biological behavior of amphiphilic molecules: the case study of molecular immunomodulators Sulfavants

Laura Fioretto,[2] Marcello Ziaco,[3] Carmela Gallo,[1] Genoveffa Nuzzo,[1] Giuliana d'Ippolito,[1] Pietro Lupetti,[4] Eugenio Paccagnini,[4] Mariangela Gentile,[4] Marina DellaGreca,[5] Marie-Sousai Appavou,[6] Luigi Paduano,[5] Raffaele De Palma,[1,7] Angelo Fontana,[1,8*] Emiliano Manzo[1*]

1 Bio-Organic Chemistry Unit, CNR-Institute of Biomolecular Chemistry, Via Campi Flegrei 34, 80078 Pozzuoli, Napoli, Italy.
2 Consorzio Italbiotec, Via Fantoli, 16/15, 20138, Milano, Italy
3 BioSearch Srl., Villa Comunale c/o Stazione Zoologica "A. Dohrn" 80121 Napoli, Italy
4 Department of Life Sciences, University of Siena, San Miniato, 53100 Siena, Italy
5 Department of Chemical Sciences, University of Naples Federico II, via Cinthia 4, 80136 Napoli, Italy
6 Jülich Centre for Neutron Science JCNS at Heinz Maier-Leibnitz Zentrum, Forschungszentrum, Jülich, 52428 Jülich, Germany
7 Medicina Interna, Immunologia Clinica e Medicina Traslazionale, Università di Genova and IRCCS-Ospedale S. Martino, 16131 Genova, Italy
8 University of Naples Federico II, Dept. of Biology, Via Cinthia – Bld. 7, 80126 -Napoli, Italy
*Correspondence email: emanzo@icb.cnr.it or afontana@icb.cnr.it

ABSTRACT: Sulfavant A and Sulfavant R, sulfoquinovoside-glycerol lipids under study as vaccine adjuvants, structurally differ only for the configuration of glyceridic carbon, *R/S* and *R* respectively. The *in vitro* activity of these substances follows a bell-shaped dose-response curve, but Sulfavant A gave the best response around 20 μM, while Sulfavant R at 10 nM. Characterization of aqueous self-assembly of these molecules by a multi-technique approach clarified the divergent and controversial biological outcome. Supramolecular structures were present at concentrations much lower than critical aggregation concentration for both products. The kind and size of these aggregates varied as a function of the concentration differently for Sulfavant A and Sulfavant R. At nanomolar range, Sulfavant A formed cohesive vesicles, while Sulfavant R arranged in spherical micellar particles whose reduced stability was probably responsible for an increase of monomer concentration in accordance with immunomodulatory profile. Instead, at micromolar concentrations transition from micellar to vesicular state of Sulfavant R occurred and thermodynamic stability of the aggregates, assessed by surface tensiometry, correlated with the bioactivity of Sulfavant A at 20 μM and the complete loss of efficacy of Sulfavant R. The study of Sulfavants provides clear evidence of how self-aggregation, often neglected, and the equilibria between monomers and aqueous supramolecular forms of lipophilic molecules deeply determine the overall bio-response.

Keywords: Sulfavants; colloid; aggregates; fluorescence; cryo-TEM; biological activity; immune response

INTRODUCTION

A large number of pharmacologically active compounds are amphiphilic molecules prone to assemble in aqueous environment spontaneously. Self-aggregation occurs by coordination processes arranging single monomers in supramolecular structures stabilized by non-covalent interactions.[1] For non-polar molecules, these interactions are driven by reduction of the thermodynamically unfavorable contact between hydrophobic structures and polar surrounding. The phenomenon of aggregation is regulated by complex equilibria among various chemo-physical states comprising both monomers and larger supramolecular structures.[2] These processes depend on several factors ranging from structural features of the molecules to environmental parameters including solute concentrations, pH, temperature, and ionic strength.[3]

Pharmacological effects of amphiphilic drugs generally occur at concentrations below the critical aggregation concentration (CAC), defined as critical micellar concentration (CMC) for micelle aggregates.[4] However, even at very low concentrations, self-assembly can affect the biological activity by changing the effective availability of free molecules that interact with the cellular targets. Consequently, any chemo-physical factor able to modify the balance between monomers and aggregates can change the overall biological activity even in *in vitro* tests. In this regard, dose-response curves represent a direct measurement of the effect of supramolecular aggregation on the biological activity over a range of concentrations. In this context, the conventional sigmoidal dose-response curves of amphiphilic drugs and drug candidates are superseded by bell-shaped curves that are characterized by the decrease of activity above the critical aggregation concentration (CAC).[5] Furthermore, although monomers are crucial for the biological efficacy of these substances and for a comparison of the therapeutic potential[6], assessment of the monomer concentration is usually hampered by the spontaneous and uncontrollable processes of aggregation under physiological conditions.

Here we aim at deciphering the correlation between *in vitro* biological activity and self-aggregation of Sulfavant A (**1**) and Sulfavant R (**2**), sulfoquinovose-based lipids that are under preclinical study as novel adjuvants of vaccines.[7,8] The study addresses the complex equilibria affecting the final state of aggregation of these products in water, and, consequently, the effective concentration of the active forms of lipophilic small molecules during cell-based assays. Analysis of supramolecular assembly in biological studies is often hindered by the co-occurrence of more than one form of aggregation and by the difficulty of measuring them at the low concentrations where the therapeutic candidate molecules show activity. For these reasons, we adopted a multi-technique approach to measure the aggregation from nanomolar to micromolar activity.

MATERIALS AND METHODS

General procedure

NMR spectra were recorded on a Bruker DRX-600 equipped with a TXI CryoProbe in $CDCl_3$, $CD_3OD/CDCl_3$ (1/1), CD_3OD and D_2O (δ values are referred to $CHCl_3$, CH_3OH and H_2O at 7.26, 3.34 and 4.79 ppm respectively). The surface tension was measured with a Sigma 70 tensiometer (KSV, Stockholm, Sweden) using the Du Noüy ring method. Light phase contrast microscopy images of Sulfavant A were recorded with Axio Vert.A1 microscope (Carl Zeiss) with magnification at 40x. Fluorescence intensity at 25 °C was measured using an FP-8300 fluorometer (Jasco, Easton, MD). Excitation wavelength at 358 nm; emission wavelength at 430 nm.

All the reagents were purchased from Sigma-Aldrich and used without any further purification.

CAC determination by surface tension

A 0.3 mM aqueous solution of Sulfavant A or Sulfavant R (in Millipore water filtered on 0.22 μm pore size syringe filter) was sonicated for 40 minutes at 35 °C. Small amounts of this solution were gradually diluted in the vessel with a known volume of water, in order to evaluate the tension surface in a range of concentration between 0.02 μM and 100 μM.

Rigorous stirring accompanied by a10 min gap, in order to equilibrate the system after each addition, was followed by surface tension measures at 25 °C by a Sigma 70 tensiometer (KSV, Stockholm, Sweden) and using the Du Noüy ring method. The CACs were obtained as an average of three measurements.

Effect of detergent agents on ^{1}H NMR spectrum of Sulfavant A and Sulfavant R

4.25 μg of Sulfavant A or Sulfavant R were dissolved in 1 mL of D_2O. Each suspension was sonicated for 40 minutes at 35°C. After 24 h, the ^{1}H NMR spectrum were recorded. At these samples 1.5 μL of a solution of Triton X100 0.17 M was added and the solutions were sonicated for 15 minutes and after 24h the ^{1}H NMR spectrum was recorded.

Sample preparation for detection of the effect of detergent agents on the biological activity of Sulfavant A

100 ng of Kolliphor RH40 were added to 0.01 μM, 0.1 μM, 1 μM, 10 μM solutions of Sulfavant A in a total volume of 1 ml of PBS.

Optical microscopy analysis

Solutions at 0.1 μM, 0.2 μM and 10 μM of Sulfavant A (**1**) and R (**2**) were prepared in 1 mL of Millipore water filtered on 0.22 μm filter. The samples were sonicated for 40 minutes at 35 °C. Images were taken at 24 h.

CAC determination by fluorescence spectroscopy:

10 μL of 0.5 mM DPH dissolved in THF were added to different solutions of Sulfavant A or Sulfavant R, in a range of concentration between 0.05 μM and 500 μM, in a total volume of 1 ml of Millipore water filtered on 0.22 μm pore size syringe filter. Before adding DPH, Sulfavant A or R solutions were sonicated for 40 minutes at 35 °C, and then tubes were incubated for 1 h in the dark at room temperature before measurement of fluorescence. The experiments were carried out in triplicate and average fluorescence was reported.

Cryo-TEM analysis

Solutions at 10 nM and 10 μM of Sulfavant A (**1**) and R (**2**) were prepared in 1 mL of Millipore water filtered on 0.22 μm filter. The samples were sonicated for 40 minutes at 35 °C and after 24h the cryo-TEM images were acquired.

For cryo-TEM analysis the samples were prepared by placing a drop of 5 microliter solution on a Quantifoil Multi A holey carbon-coated copper grid (copper R2/1, Quantifoil Micro Tools GmbH) that were previously glow discharged. Excess fluid was blotted from the grid and plunge frozen in liquid ethane using a FEI Vitrobot Mark IV plunge freezer to achieve sample vitrification. Frozen samples were stored in liquid nitrogen until EM imaging in a Philips CM200FEG microscope equipped with a TVIPS TemCam-F224HD CCD camera and a Gatan 626 Cryo-Holder. Parallel analysis were performed on a JEM 2200 FS EFTEM instrument (JEOL, Tokyo, Japan). Examinations were carried out at temperatures around -180°C. The transmission electron microscope was operated at an acceleration voltage of 200 kV. Zero-loss filtered images were taken under reduced dose conditions (<10 000 e-/nm2). All images were recorded digitally by a bottom-mounted 16 bit CMOS camera system (TemCam-F216, TVIPS, Munich, Germany). To avoid any saturation of the gray values, all the measurements were taken with intensity below 15 000, considering that the maximum value for a 16 bit camera is 2^16. Images have been taken with EMenu 4.0 image acquisition program (TVIPS, Munich, Germany) and processed with a free digital imaging processing system Image J.[9,10]

Human monocyte-dendritic cell differentiation.

Human peripheral blood mononuclear cells were isolated from two healthy donors by routine Ficoll density gradient centrifugation. Monocytes were purified from human peripheral blood mononuclear cells using MACS CD14 microbeads (Miltenyi Biotech, Auburn, CA) according to the manufacturer's recommendation. Purity was checked by staining with a FITC-conjugated anti-CD14 antibody (Milteny Biotech) and FACS analysis and was routinely found to be greater than 98%. Immature DCs were obtained by incubating monocytes at $7 \cdot 10^5$ cell/mL in RPMI 1640 medium supplemented with 10% fetal calf serum, 1% L-glutamine 2mM, 1% penicillin and streptomycin, human IL-4 (5 ng/mL) and human GM-CSF (100 ng/mL) for five days.

Cells Staining and stimulation.

After five days in culture, surface staining was performed on monocyte-derived dendritic cells for flow cytometry analysis. moDCs were stained by using the following conjugated antibody from Milteny Biotech: HLA-DR FITC, CD83 PE, CD86 APC, CD54 PE Vio770, and analyzed by flowcytometer (BD LSRFortessa X-20, BD Bioscience, Milano, Italy) according to standard protocol. moDCs were then incubated with synthetic compounds in 12-wells at concentration of $7 \cdot 10^5$ cell/mL. Stimulation with PAM2CSK4 1μg mL^{-1} (Invivogen) was used as positive control. After 24 hours, expression of all surface markers was estimated again by fluorochrome-conjugated antibodies.

For experiments with Kolliphor RH40 (Sigma Aldrich), a titration curve of hDCs treated with an increased amount of detergent from 0.026 nM to 2.6 μM was set up for the establishment of the concentration that does not affect cell maturation and vitality. All the experiments were then performed by dissolving Sulfavant A in a 260 nM detergent solution in PBS and 10 μL of this solution was added to each well, by reaching a final concentration of 2.6 nM of Kolliphor RH40.

RESULTS AND DISCUSSION

Synthetic β-6'-sulfoquinovosyldistearoylglycerols (β-SQDGs) are negatively charged lipids showing unusual immunomodulatory activity.[7,8] The prototype of this class, Sulfavant A (**1**),[7,8] [1,2-*O*-distearoyl-3-*O*-(β-sulfoquinovosyl)-*R/S*-glycerol], exhibits the ability to modulate activation of antigen-presenting cells (APCs), such as human dendritic cells (DCs), and trigger immune response both in *in vitro* and *in vivo* experiments.[8a] DCs coordinate both innate and adaptive immunity thus the ability of Sulfavant A (**1**) to stimulate these cells opened the way to the development of a new chemical family of vaccine adjuvants and immunomodulators.

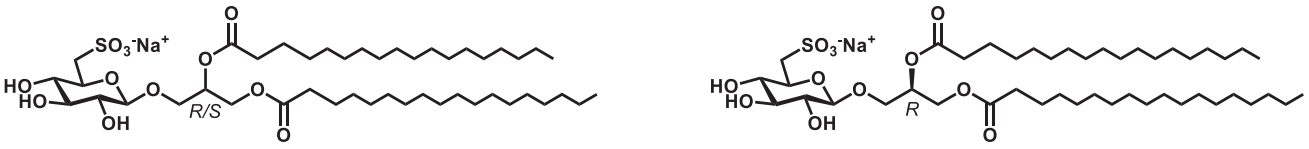

Chemical structures of Sulfavant A (**1**) and Sulfavant R (**2**)

Sulfavant A is a mixture of *R/S* epimers at carbon 2 of the glycerol moiety while Sulfavant R (**2**)[7] is the enantiopure *R* analog. Despite the very similar chemical structures, the latter compound induced maturation of hDC at nanomolar concentrations (≈10 nM) while the parent molecule **1** showed the highest activity only at micromolar concentrations (10-30 μM).[7] This divergent response is correlated to the amphiphilic nature of these products that tend to form supramolecular aggregates in aqueous solution as we previously underlined by dynamic light scattering (DLS) measurements displaying different hydrodynamic radius for **1** (about 150 nm) and **2** (about 50 nm).[7,8d]

For the characterization of spontaneous aggregation of amphiphilic products in water, a diagnostic parameter is the critical aggregation concentration (CAC).[5,11] At the CAC, free monomers aggregate to form supramolecular structures.[2a,12,13] Consequently, for high cooperative self-aggregation, CAC represents the highest concentration of monomer in solution. This parameter is also a key determinant of the properties of amphiphilic substances as it shows the natural tendency to self-aggregate[2,12-14] and the break point above which a marked change of the physico-chemical properties of the suspension occurs.[2,12-14] Surface tension analysis of Sufavant A (**1**) and R (**2**) revealed significantly different CACs with values of 70 μM and 15 μM respectively (Supporting Information). As CAC is related also to change in the Gibbs free energy of the aggregation process ($\Delta G°_{agg}$), the thermodynamic stability of supramolecular aggregates was calculated as:

$\Delta G°_{agg}$ (**1**) = -24.1 kJ/mol (eq. ***1***)

$\Delta G°_{agg}$ (**2**) = -27.5 kJ/mol (eq. ***2***)

These values indicated that, at micromolar concentration, the aggregation process of Sulfavant A (**1**) was less favored than that of Sulfavant R (**2**), confirming not only the evidence about the difference between the physico-chemical properties of these products in water suspension, but also a more cohesive nature of Sulfavant R aggregates compared to those of Sulfavant A in this concentration range. However, if for Sulfavant A (**1**) a CAC of 70 μM agrees with the bell-shaped dose-response curve that shows a decrease of the activity at concentration higher than 60 μM, the results are not consistent with the activity

of Sulfavant R (**2**), which has a maximum of the bell-shaped activity at 10 nM, a concentration 1000-fold lower than its CAC.

As biological mechanisms such as action on different cellular targets can be excluded (manuscript in preparation), possible explanations for these differences lie in the physico-chemical behavior of these small molecules below CAC. Furthermore, while there is a general consensus that the self-association of organic molecules into colloidal particles can drastically change their biological response, the investigation at concentrations much lower than CAC has so far received little attention.[15] In particular, the experimental evidence points toward the presence of aggregates even at very low concentration, which is not unusual for amphiphilic molecules that show less cooperative aggregation tendency. Thus, to investigate on the presence of aggregates in low concentration solutions, we tested the effects of detergents (disaggregating agents) on aqueous suspensions of **1** and **2** at concentrations lower than CAC by ^{1}H-NMR[16] (Figure 1).

Line broadening and loss of resolution of the NMR signals are due to the slowing down of the molecular movements and change of the relaxation time following aggregation.[16b] Triton X100 was selected as a detergent because the signals of the molecule did not show overlapping with those diagnostic ones of Sulfavants. In organic solvent ($CDCl_3/CD_3OD$ 1:1 v/v), the lowest concentration that permit a clear detection of the ^{1}H-NMR signal of **1** and **2** was 5 μM. At the same concentration, no signal could be detected in D_2O because of the supramolecular assembling. As shown with the glyceridic methine proton at 5.24 ppm and the anomeric proton at 4.33 ppm in Figure 1, stepwise addition of Triton X100 determined recovery of the signals due to the partial disruption of aggregation that was linearly dependent on the concentration of the detergent. The experiment clearly proved that the supramolecular association was already in place at concentrations lower than CAC as calculated by surface tension measurements.

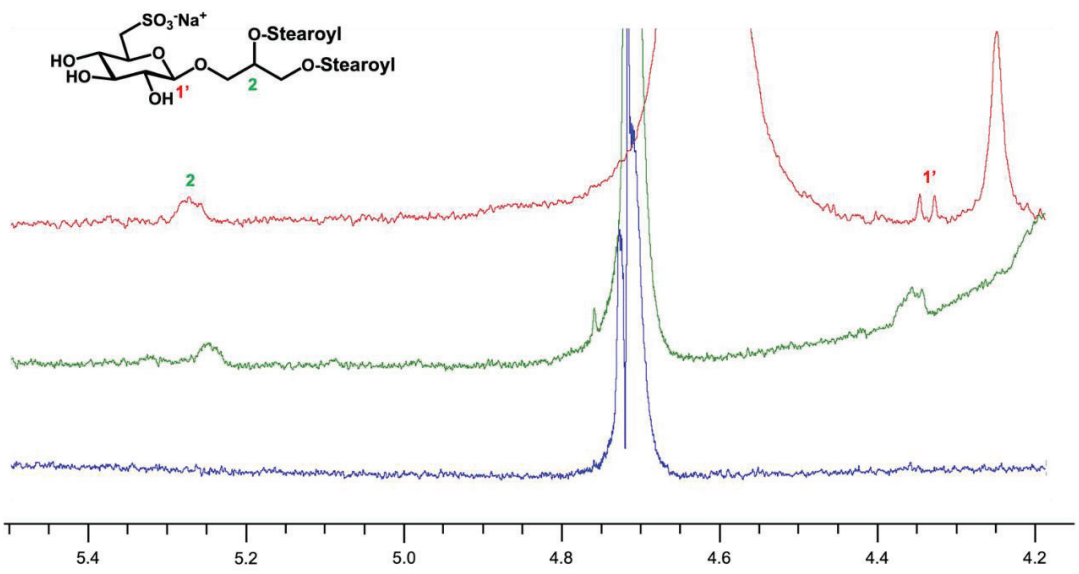

Figure 1. Region of the ^{1}H-NMR spectra of Sulfavant A (**1**) at 5 μM in $CDCl_3/CD_3OD$ 1/1 (red line), in D_2O with (green line) and without (blue line) 0.26 μM Triton X100.

The same results were obtained for Sulfavant R (**2**) (Supporting information) and suggested that these physical behaviors are responsible for the points where the immunomodulatory activity of Sulfavants reaches a plateau or even begins to drop. To corroborate these results, we tested the effect of the addition of a detergent on the role of Sulfavant A (**1**) in increasing the expression of the co-stimulatory marker CD83, [7,8] a surface glycoprotein that is strongly up-regulated during hDC maturation and for this reason one of main hDC maturation signs. Triton X100 is toxic to hDCs and we replaced it with the nonionic emulsifying agent Kolliphor RH 40[17] that alone didn't impact on hDCs maturation. The addition of 2.6 nM of this detergent to water suspensions of **1** induced a significant increase of the potency from 20 μM to 100 nM, even if the dose-response curve maintained the characteristic bell shape (Figure 2). The results with Kolliphor RH 40 confirmed that the potency of Sulfavant A (**1**) on hDC maturation was affected by supramolecular aggregation, as well as suggested the formation of spontaneous association below the calculated CAC. The same experiment performed on Sulfavant R (**2**) did not show any shift of nanomolar centered activity curve (Supporting Information), probably due to quite disaggregated state of this compound at this concentration range.

The NMR evidence of the formation of aggregates below 5 μM implied that the surface tension measurements were only indicative of an apparent CAC and well below to this value, aggregates are present. These structures are not unusual with lipophilic anionic substances[18] and are visible with Sulfavant A (**1**) by light phase contrast microscopy above 100 μM (Supporting Information).

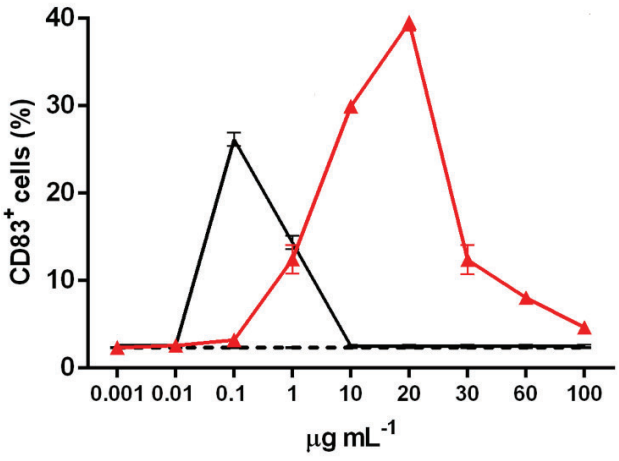

Figure 2. Percentage of mature $CD83^+$ cells after stimulation by Sulfavant A (**1**) without (red line) and with (black line) Kolliphor RH40 as detergent,Data are expressed as mean and standard deviation from a duplicate of two independent experiments.

In order to confirm the presence of aggregated structures below CAC and to evaluate the real concentration at which monomers of **1** and **2** start assembling, we applied a fluorescent method based on 1,6-diphenyl-1,3,5-hexatriene (DPH), a probe usually used in these kinds of experiments.[19] Intensity and wavelength of fluorescent emission depends in fact on the surrounding environment.

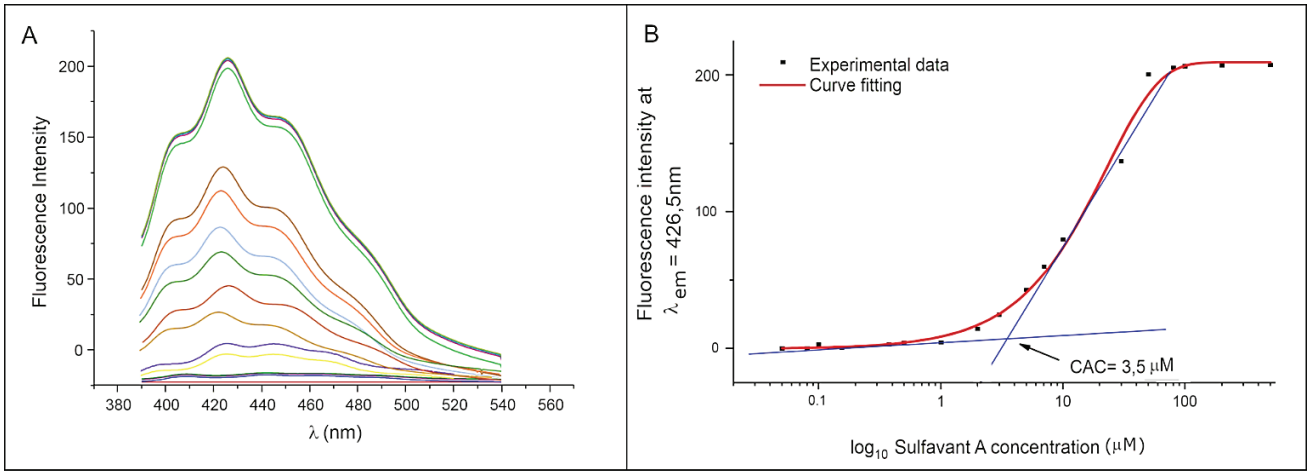

Figure 3. Study of the aggregation of Sulfavant A (**1**) by fluorescence analysis between 0.05 µM and 500 µM. (A) Dependence of the fluorescent emission bands of DPH with different concentration of **1**; (B) Critical aggregation concentration (CAC) determined by analysis of the fluorescence data.

Below and above aggregation, a lipophilic fluorescent probe is surrounded by polar (water) and apolar (aggregates) domains that modify the optical properties. In this regard, 1,6-diphenyl-1,3,5-hexatriene (DPH) does not have emission in water[19c] but it shows intense emission wavelengths at 426.5 nm when incorporated into apolar aggregates. The fluorescence analysis of DPH emission as a function of the concentration of Sulfavant A (**1**) is reported in Figure 3. The results showed spontaneous aggregation already at a concentration of 3.5 µM. Identical results were recorded with Sulfavant R (**2**) (Supporting Information). It is worth noting that the fluorescence analysis for measurements below 1 µM did not involve any substantial changing in the fluorescence intensity.

Therefore, although the presence of lower concentration aggregates could not be ruled out, these results highlighted that the assessment of the aggregation of Sulfavants in water was dependent on the sensitivity of the technique used for the analysis. In this regard, cryogenic transmission electron microscopy (Cryo-

TEM) represents the most sensitive approach for the study of nanostructures in a diluted aqueous solution.[20] Differently from other microscopy methods, the technique combines high resolution and sensitivity of electron microscopy with the preservation of the self-assembled structures. Cryo-TEM relies on a rapid drop of temperature to convert the solvent to a solid glass and instantly freeze the putative nanostructures. It does not require the addition of stabilizers and contrast enhancers, or the dehydrating/embedding treatments routinely used for the preparation of the samples at room temperature.[21] As shown in Figure 4, Cryo-TEM permitted direct imaging of aqueous solutions of Sulfavant A (**1**) and Sulfavant R (**2**) in the range of the immunomodulatory activity of these products, between nanomolar and micromolar concentrations.

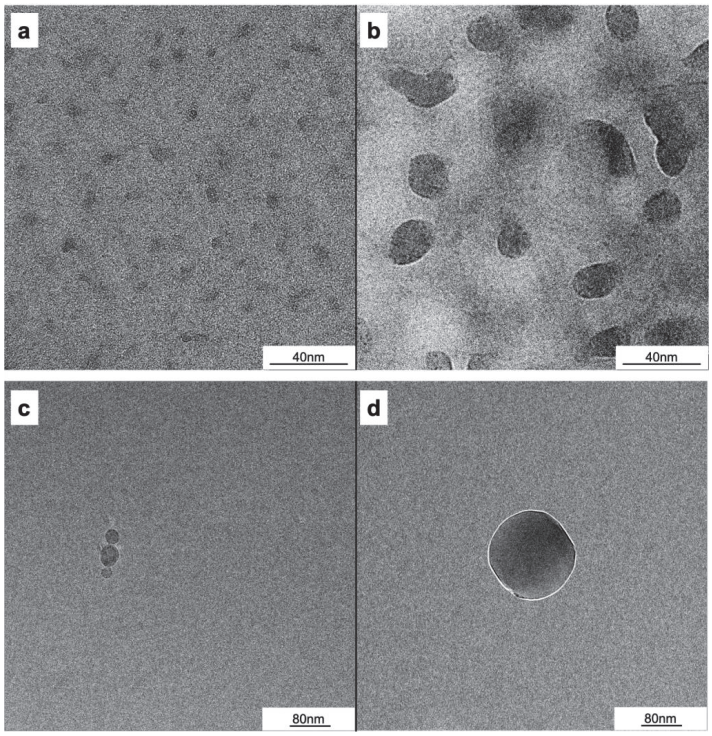

Figure 4. Cryo-TEM images of Sulfavants in water. (A) Sulfavant R (**2**) at 10 nM; (B) Sulfavant A (**1**) at 10 nM; (C) Sulfavant R (**2**) at 10 μM; (D) Sulfavant A (**1**) at 10 μM

At 10 nM, the Cryo-TEM microscopy revealed spherical micellar particles of approximately 3-5 nm for Sulfavant R (Figure 4a), while the images of Sulfavant A (**1**) showed spontaneous assembly in colloidal vesicles of approximately 30-40 nm (Figure 4b). Given the dynamic nature of micelles compared to more structured and stable vesicles,[22] the analysis agreed with the fact that only Sulfavant R (**2**) was active at this concentration. In contrast, microscope images at 10 μM showed that Sulfavant R (**2**) aggregated in spherical vesicles of about 30-40 nm (Figure 4c), while Sulfavant A (**1**) formed bigger vesicular structures of about 150-160 nm (Figure 4d). Overall, the data supported a concentration-dependent increase of the

particle size with both molecules, as well as the transition from micellar to vesicular form of **2**. The Cryo-TEM results also suggested that the biological activity of these compounds was associated to monomers or very small aggregates (dimers/trimers) while the supramolecular structures were less involved in the interaction with the cellular targets. As reported above (eq. ***1*** and eq. ***2***), surface tension measurements indicated that aggregation of Sulfavant A (**1**) is less favorable than that of Sulfavant R (**2**) at micromolar concentrations [$\Delta G°_{agg.}$ (**2**) < $\Delta G°_{agg.}$ (**1**)]. Therefore, in agreement with the experimental data, the monomer concentration of **1** should be higher and enough to trigger the biological response above 10 μM. On the other hand, the 30-40 nm vesicles of Sulfavant R (**2**) are more cohesive and this product is not active at 10 μM because monomer (or dimers/trimers) concentrations didn't reach the bioactivity values, differently from the less cohesive Sulfavant A aggregates.

CONCLUSIONS

Sulfavant A (**1**) and Sulfavant R (**2**) are amphiphilic molecules differing only for the configuration of the oxymethine carbon of glycerol that is *R*/*S* in **1** and *R* in **2**. Despite the very close structural similarity, these products displayed a significantly different immunomodulatory activity depending on the organization and stability of their supramolecular structures in aqueous solutions. As summarized in Figure 5, the results of the multi-technique analysis, based on surface tensiometry, dynamic light scattering (DLS), nuclear magnetic resonance (NMR), fluorescence light phase contrast and cryo-electron microscopy, suggest that more equilibrium between the aggregates and the free monomers are responsible for the biological activity of these products. These equilibria occur below the CAC and their assessment is crucial for a comparative test of the preliminary therapeutic development of Sulfavants. In our opinion, this response could be common to other lipophilic and amphiphilic compounds, such as natural products, lipopeptides, and glycolipids, whose activity can be significantly affected by supramolecular self-assembly in aqueous media. This aspect has been often neglected but the study of Sulfavants demonstrates that evaluation of the biological potential of similar products can be strictly dependent on a careful assessment of the somehow unpredictable chemical-physical processes during biological tests.

To the best of our knowledge, there are no other reports on the influence of a single stereocenter on the aggregation as in the case of **1** and **2**. Thus, in addition to the preclinical development as adjuvants and innate immune modulators, these compounds can offer a new opportunity to study the mechanisms of self-assembly of lipophilic products in aqueous media.

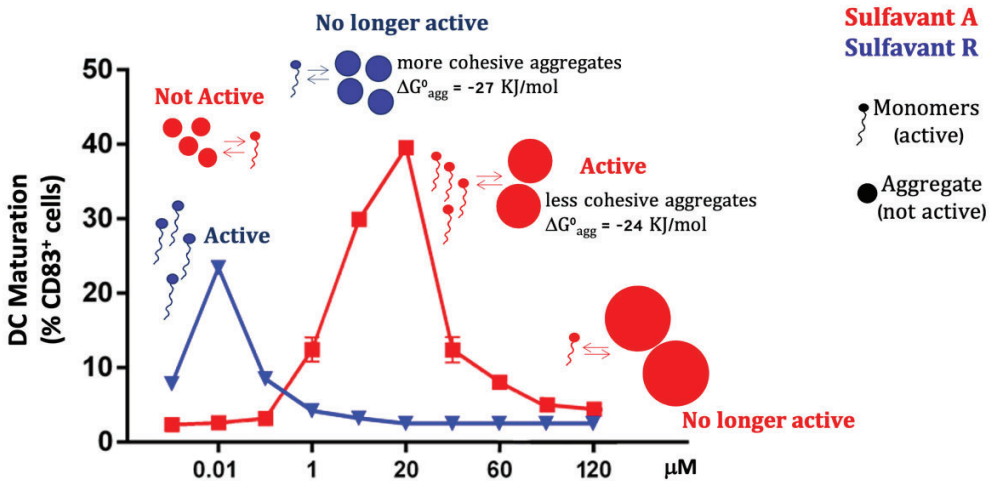

Figure 5. Correlation between Sulfavant A (red line) and Sulfavant R (blue line) self-assembling and their biological activity

ASSOCIATED CONTENT

Supporting Information

The Supporting Information includes: the tension surface curves of Sulfavant A (**1**) and Sulfavant R (**2**); the ^{1}H-NMR spectra of Sulfavant R (**2**) at 5 μM with and without Triton X100; the percentage of mature CD83^{+} cells after stimulation by Sulfavant R (**2**) with and without Kolliphor RH40; light phase contrast microscopy images of Sulfavant A aqueous solution at 0.1 mM and 0.2 mM and the critical aggregation concentration (CAC) of Sulfavant R determined by analysis of the fluorescence data.

AUTHOR INFORMATION

Corresponding Authors

Emiliano Manzo - *Bio-Organic Chemistry Unit, CNR-Institute of Biomolecular Chemistry, Via Campi Flegrei 34, 80078 Pozzuoli, Napoli, Italy;*

Email: emanzo@icb.cnr.it

Angelo Fontana - *Bio-Organic Chemistry Unit, CNR-Institute of Biomolecular Chemistry, Via Campi Flegrei 34, 80078 Pozzuoli, Napoli, Italy*; University of Naples Federico II, Dept. of Biology, Via Cinthia – Bld. 7, 80126 -Napoli, Italy;

Email: afontana@icb.cnr.it

Authors

Laura Fioretto - *Italbiotec*, Via Fantoli, 16/15, 20138, Milano, Italy / *Bio-Organic Chemistry Unit, CNR-Institute of Biomolecular Chemistry, Via Campi Flegrei 34, 80078 Pozzuoli, Napoli, Italy*. Email: l.fioretto@icb.cnr.it

Marcello Ziaco - *BioSearch Srl., Villa Comunale c/o Stazione Zoologica "A.Dohrn" 80121 Napoli, Italy*; Email: m.ziaco@icb.cnr.it

Carmela Gallo - *Bio-Organic Chemistry Unit, CNR-Institute of Biomolecular Chemistry, Via Campi Flegrei 34, 80078 Pozzuoli, Napoli, Italy*; Email: carmen.gallo@icb.cnr.it

Genoveffa Nuzzo - *Bio-Organic Chemistry Unit, CNR-Institute of Biomolecular Chemistry, Via Campi Flegrei 34, 80078 Pozzuoli, Napoli, Italy*; Email: nuzzo.genoveffa@icb.cnr.it

Giuliana d'Ippolito - *Bio-Organic Chemistry Unit, CNR-Institute of Biomolecular Chemistry, Via Campi Flegrei 34, 80078 Pozzuoli, Napoli, Italy*; Email: gdippolito@icb.cnr.it

Pietro Lupetti - *Department of Life Sciences, University of Siena, San Miniato, 53100 Siena, Italy*; Email: pietro.lupetti@unisi.it

Eugenio Paccagnini - *Department of Life Sciences, University of Siena, San Miniato, 53100 Siena, Italy*; Email: eugenio.paccagnini@unisi.it

Mariangela Gentile - *Department of Life Sciences, University of Siena, San Miniato, 53100 Siena, Italy*; Email: mariangela.gentile@unisi.it

Marina DellaGreca - *Department of Chemical Sciences, University of Naples Federico II, via Cinthia 4, 80136 Naples, Italy*; Email: dellagre@unina.it

Marie-Sousai Appavou - Jülich Centre for Neutron Science, Forschungszentrum Jülich, 52428 Jülich, Germany; Email: m.s.appavou@fz-juelich.de

Luigi Paduano - *Department of Chemical Sciences, University of Naples Federico II, via Cinthia 4, 80136 Naples, Italy*; Email: lpaduano@unina.it

Raffaele De Palma - *Clinica di Medicina Interna, Immunologia Clinica e Medicina Traslazionale, Ospedale S. Martino, Genova, Italy*; Email: raffaele.depalma@unige.it

Notes

The authors declare no competing financial interest.

Author Contributions

The manuscript was written through contributions of all authors. All authors have given approval to the final version of the manuscript.

Funding Sources

This work was supported by the project "Antitumor Drugs and Vaccines from the Sea (ADViSE)" project (CUP B43D18000240007 – SURF 17061BP000000011) funded by POR Campania FESR 2014-2020 "Technology Platform for Therapeutic Strategies against Cancer" - Action 1.1.2 and 1.2.2.

Notes

The authors declare no ethical issue.

ACKNOWLEDGMENT

AF and EM thank "Antitumor Drugs and Vaccines from the Sea (ADViSE)" project (CUP B43D18000240007 – SURF 17061BP000000011) and BioSEArch SRL for the generous support; EM and LF wish to thank European Union (FSE, PON Ricerca e Innovazione 2014-2020, Azione I.1 "Dottorati Innovativi con caratterizzazione Industriale"), for funding a Ph.D. grant to one of the authors (Laura Fioretto).

Marie-Sousai Appavou thanks the EU□H2020 research and innovation program under grant agreement No 654360, having benefited from the access provided by the Jülich Centre for Neutron Science at Maier-Leibnitz-Zentrum in Garching, Germany within the framework of the NFFA-Europe Transnational Access Activity.

The authors would like to thank Dr. Lucio Caso (CNR-ICB) for the technical support in most of the steps of this research.

REFERENCES

(1) Lehn, J.M. Toward self-organization and complex matter. *Science* **2002** 295, 2400-2403.

(2) (a) Coan, K. E.; & Shoichet, B. K. Stoichiometry and physical chemistry of promiscuous aggregate-based inhibitors. *Journal of the American Chemical Society* **2008**, *130*(29), 9606-9612; (b) Corkvill, J.M.; Goodman, J.F.; Harrold, S.P. Thermodynamics of micellization of non-ionic detergents. *Transactions of the Faraday Society* **1964**, 60, 202-208; (b) Corkvill, J.M.; Goodman, J.F.; Walker, T.; Wyer, J. The multiple equilibrium model of micelle formation. *Proceedings of the Royal Society of London. A. Mathematical and Physical Sciences* **1969,** 312, 243-255.

(3) (a) Israelachvili, J.N. *Intermolecular and Surface Forces* (III Ed). Academic Press **2011**; (b) Yang, Y.; Dong, J.; li, X. Micelle to vesicle transitions of N- dodecyl-1, o-diaminoalkanes: Effect of pH, temperature and salt. *Journal of Colloid and Interface Science* **2012**, 380, 83-89; (c) Jiang, Z.; Liu, J.; Sun,

K.; Dong, J.; Li, X.; Mao, S.; Du, Y.; Liu, M. pH- and concentration-induced micelle-to-vesicle transitions in pyrrolidone-based gemini surfactants. *Colloid and Polymer Science* **2014**, 292, 739-747.

(4) Attwood, D.: Florence, A.T. Surfactant Systems, Chapman and Hall, London **1983**

(5) (a) Owen, S.C.; Doak, A.K.; Ganesh, A.N.; Nedyalkova, L.; McLaughlin, C.K.; Shoichet, B.K.; Shoichet, M.S. Colloidal Drug Formulations Can Explain "Bell-Shaped" Concentration-Response Curves. *ACS chemical biology* **2014**, 9, 777-784; (b) Owen, S.C.; Doak, A.K.; Wassam, P.; Shoichet, B.K. Colloidal Aggregation Affects the Efficacy of Anticancer Drugs in Cell Culture. *ACS chemical biology* **2012** 7, 1429-1435.

(6) (a) Wang, J. Solubility at the Molecular Level: Development of a Critical Aggregation Concentration (CAC) Assay for Estimating Compound Monomer Solubility. *Pharmaceutical research* **2012** 29, 1745-1754; (b) Danov, K.D.; Kralchevsky, P.A.; Ananthapadmanabhan, K.P. Micelle-monomer equilibria in solutions of ionic surfactants and in ionic-nonionic: A generalized phase separation model. *Advances in colloid and interface science* **2014** 206, 17-45.

(7) Manzo, E.; Gallo, C.; Fioretto, L.; Nuzzo, G.; Barra, G.; Pagano, D.; Russo Krauss, I.; Paduano, L.; Ziaco, M.; DellaGreca, M.; De Palma, R.; Fontana, A. Diasteroselective colloidal self-assembly affects the immunological response of the molecular adjuvant Sulfavant. *ACS Omega* **2019**, 4 (4), 7807-7814.

(8) (a) Manzo, E.; Cutignano, A.; Pagano, D.; Gallo, C.; Barra, G.; Nuzzo, G.; Sansone, C.; Ianora, A.; Urbanek, K.; Fenoglio, D.; Ferrera, F.; Bernardi, C.; Parodi, A.; Pasquale, G.; Leonardi, A.; Filaci, G.; De Palma, R.; and Fontana, A. A new marine-derived sulfoglycolipid triggers dendritic cell activation and immune adjuvant response. *Scientific Reports* **2017** 7, 6286; (b) Manzo, E.; Fioretto, L.; Pagano, D.; Nuzzo, G.; Gallo, C.; De Palma, R.; Fontana, A. Chemical synthesis of marine-derived sulfoglycolipids, a new class of molecular adjuvants. *Marine Drugs* **2017**, 15 (9), 288; (c) Manzo, E.; Ciavatta, M.L.; Pagano, D.; Fontana, A. An efficient and versatile chemical synthesis of bioactive glycoglycerolipids. *Tetrahedron Letters* **2012**, 53, 879-881; (d) Manzo, E.; Fioretto, L.; Gallo, C.; Ziaco, M.; Nuzzo, G.; D'Ippolito, G.; Borzacchiello, A.; Fabozzi, A.; De Palma, R.; Fontana, A. Preparation, Supramolecular Aggregation and Immunological. Activity of the Bona Fide Vaccine Adjuvant Sulfavant S. *Marine Drugs* **2020**, 18 (9), 451; (e) Ziaco, M.; Fioretto, L.; Nuzzo, G.; Fontana, A.; Manzo, E. A short gram-scale synthesis of Sulfavant A. *Organic Process Research & Development* **2020**, 24(11), 2728-2733.

(9) Schneider, C.A.; Rasband, W.S.; Eliceiri, K.W. NIH Image to ImageJ: 25 years of image analysis. *Nature Methods* **2012**, 9, 671-675.

(10) Abramoff, M.D.; Magalhaes, P.J.; Ram, S.J. Image Processing with ImageJ. *Biophotonics International* **2004**, 11 (7), 36-42.

(11) Aurell, C.A.; Wistrom, A.O. Critical Aggregation Concentrations of Gram-Negative Bacterial Lipopolysaccharides (LPS). *Biochemical and biophysical research communications* **1998**, 253 (1), 119-123.

(12) (a) Hunter, R.J. Foundations of Colloid Science. Oxford University Press: New York, chapter 10 **1991**; (b) Cai, X.; Yang, W.; Huang, L.; Zhu, Q.; Liu, S. A series of sensitive and visible fluorescence-turn-on probes for CMC of ionic surfactants: Design, synthesis, structure influence on CMC and sensitivity, and fast detection via a plate reader and a UV light. *Sensors and Actuators B: Chemical* **2015**, 219, 251-260; (c) Chakraborty, T.; Chakraborty, I.; Chosh, S. The methods of determination of critical concentrations of the amphiphilic systems in aqueous medium. *Arabian Journal of Chemistry* **2011**, 4, 265-270.

(13) (a) Jumpertz, T.; Tschapek, B.; Infed, N.; Smits, S.H.J.; Ernst, R.; Schmitt, L. High-throughput evaluation of the critical micelle concentration of detergents. *Analytical Biochemistry* **2011**, 408, 64-70; (b) Ganesh, A.N.; Donders, E.N.; Shoichet, B.K.; Shoichet, M.S. Colloidal aggregation: From screening nuisance to formulation nuance. Nano Today, 2018, 19, 188-200.

(14) Ruckenstein, E.; Nagarajan, R. Critical Micelle Concentration. A Transition Point for Micellar Size Distribution. *Journal of Physical Chemistry* **1975**, 79 (24), 2622-2626.

(15) (a) Mukerjee, P. Micellar properties of drugs: micellar and nonmicellar patterns of self-association of hydrophobic solutes of different molecular structures -monomer fraction, availability and misuses of micellar hypothesis. *Journal of Pharmaceutical Sciences* **1974**, 63(6), 972-981; (b) Cui, X.; Mao, S.; Liu, M.; Yuan, H.; Du, Y. Mechanism of surfactant micelle formation. *Langmuir* **2008**, 24, 10771-10775; (c) Ernandes, J.R., Chaimovich, H.; Schreier, S. Spin label study of detergents in the region of critical micelle concentration. *Chemistry and Physics of Lipids* **1977**, 18, 304-315; (d) Screier, S.; Ernandes, J.R.; Cuccovia, I.M.; Chaimovich, H. Spin label studies of structural and dynamical properties of detergent aggregates. *Journal of Magnetic Resonance* **1978**, 30, 283-298; (d) Barnadas-Rodriguez, R.; Cladera, J. Steroidal surfactants: detection of premicellar aggregation, secondary aggregation changes in micelles, and hosting of a highly charged negative substance. *Langmuir* **2015**, 31, 8980-8988; (e) Eismin, R.J.; Munusamy, E.; Kegel, L.L.; Hogan, D.E.; Maier, R.M.; Scwartz, S.D.; Pemberton, J.E. Evolution of aggregate structure in solutions of anionic monorhamnolipids: experimental and computational results. *Langmuir* **2017**, 33, 7412-7424.

(16) (a) Cerichelli, G.; Mancini, G. NMR techniques applied to micellar systems. *Current opinion in colloid & interface science* **1997**, 2(6), 641-648; (b) LaPlante, S. R., Carson, R., Gillard, J., Aubry, N., Coulombe, R., Bordeleau, S., Bonneau, P., Little, M., O'Meara, J., Beaulieu, P. L. Compound aggregation in drug discovery: implementing a practical NMR assay for chemists. *Journal of Medicinal Chemistry* **2013**, 56(12), 5142-5150.

(17) (a) Tran, T.; Rades, T.; Müllertz, A. Formulation of self-nanoemulsifying drug delivery systems containing monoacyl phosphatidylcholine and Kolliphor® RH40 using experimental design. *Asian Journal of Pharmaceutical Sciences* **2018**, 13 (6), 536-545; (b) Berthelsen, R.; Holm, R.; Jacobsen, J.; Kristensen, J.; Abrahamsson, B.; Müllertz, A. Kolliphor Surfactants Affect Solubilization and Bioavailability of Fenofibrate. Studies of in Vitro Digestion and Absorption in Rats. *Molecular Pharmaceutics* **2015**, 12

(4), 1062–1071; (c) Yamamoto, Y.; Sahara, H.; Takenouchi, M.; Matsumoto, Y.; Imai, A.; Fujita, T.; Tamura, Y.; Takahashi, N.; Gasa, S.; Matsumoto, K.; Ohta, K.; Sugawara, F.; Sakaguchi, K.; Jimbow, K.; Sato, N. Inhibition of CD62L+ T-cell response in vitro via a novel sulfo-glycolipid, β-SQAG9 liposome that binds to CD62L molecule on the cell surface. *Cellular immunology* **2004**, 232, 105-115.

(18) (a) Roy, S.; Dey, J. Spontaneously formed vesicles of sodium N-(11-Acrylamidoundecanoyl)-glycinate and L-Alaninate in water. *Lagmuir* **2005**, 21, 10362-10369; (b) Miyagishi, S.; Suzuki, H.; Asakawa, T. Microviscosity and aggregation number of potassium N-acylalaninate micelles in potassium chloride solution. *Langmuir* **1996**, 12, 2900-2905; (c) Miyagishi, S.; Kurimoto, H.; Asakawa, T. Microviscosity of sodium N-acylvalinate micelles in sodium chloride solution. *Langmuir* **1995**, 11, 2951-2956; (d) Miyagishi, S.; Akasohu, W.; Hasimoto, T.; Asakawa, T. Effect of NaCl on aggregation number, microviscosity, and cmc of N-Dodecanoyl amino acid surfactant micelles. *Journal of colloid and interface science* **1996**, 184, 527-534.

(19) (a) Brito, R. M.; Vaz, W. L. Determination of the critical micelle concentration of surfactants using the fluorescent probe N-phenyl-1-naphthylamine. *Analytical biochemistry* **1986**, 152(2), 250-255; (b) Kalyanasundaram, K. Pyrene fluorescence as a probe of fluorocarbon micelles and their mixed micelles with hydrocarbon surfactants. *Langmuir* **1988**, 4(4), 942-945; (c) London, E.; Feigenson, G. W. A convenient and sensitive fluorescence assay for phospholipid vesicles using diphenylhexatriene. *Analytical biochemistry* **1978**, 88(1), 203-211; (d) Nakahara, Y.; Kida, T.; Nakatsuji, Y.; Akashi, M. New Fluorescence Method for the Determination of the Critical Micelle Concentration by Photosensitive Monoazacryptand derivatives. *Langmuir* **2005**, 21, 6688-6695.

(20) (a) Laan, A. C.; Denkova, A. G. Cryogenic transmission electron microscopy: the technique of choice for the characterization of polymeric nanocarriers. *EJNMMI research* **2017**, 7(1), 44; (b) Franken, L. E.; Boekema, E. J.; Stuart, M. C. Transmission electron microscopy as a tool for the characterization of soft materials: application and interpretation. *Advanced Science* **2017**, 4(5), 1600476.

(21) Dubochet, J.; Adrian, M.; Chang, J. J.; Homo, J. C.; Lepault, J.; McDowall, A. W.; Schultz, P. Cryoelectron microscopy of vitrified specimens. In: *Cryotechniques in Biological Electron Microscopy;* Springer, Berlin, Heidelberg, **1987**. p. 114-131.

(22) (a) Egelhaaf, S.U.; Schurtenberger, P. Micelle-to-Vesicle Transition: A Time-Resolved Structural Study. *Physical Review Letters* **1999**, 82, 2804-2807; (b) Leng, J.; Egelhaaf, S.U.; Cates, M.E. Kinetics of the Micelle-to-Vesicle Transition: Aqueous Lecithin-Bile Salt Mixtures. *Biophysical Journal* **2003**, 85, 1624-1646. (c) Aniansson, E. A. G.; Wall, S. N.; Almgren, M.; Hoffmann, H.; Kielmann, I.; Ulbricht, W.; Zana, R.; Lang, J.; Tondre, C. Theory of the kinetics of micellar equilibria and quantitative interpretation of chemical relaxation studies of micellar solutions of ionic surfactants. *The Journal of Physical Chemistry* **1976**, 80(9), 905-922; (d) Morigaki, K.; Walde, P.; Misran, M.; Robinson, B. H. Thermodynamic and

kinetic stability. Properties of micelles and vesicles formed by the decanoic acid/decanoate system. *Colloids and Surfaces A: Physicochemical and Engineering Aspects* **2003**, 213(1), 37-44; (e) Dushkin, C. D.; Ivanov, I. B.; Kralchevsky, P. A. The kinetics of the surface tension of micellar surfactant solutions. *Colloids and Surfaces* **1991**, 60, 235-261; (f) Lasic, D. The mechanism of vesicle formation. *Biochemical Journal* **1988**, 256, 1-11.